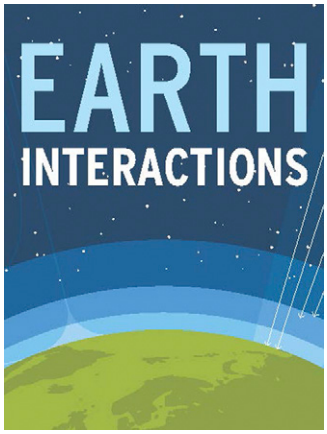

© 2018 American Meteorological Society. For information regarding reuse of this content and general copyright information, consult the AMS Copyright Policy (www.ametsoc.org/PUBSReuseLicenses).

Agro-Climate Projections for a Warming Alaska

Rick Lader[a]

Dept. of Atmospheric Sciences, Geophysical Institute, and International Arctic Research Center, University of Alaska Fairbanks, Fairbanks, Alaska

John E. Walsh

International Arctic Research Center, University of Alaska Fairbanks, Fairbanks, Alaska

Uma S. Bhatt

Dept. of Atmospheric Sciences, Geophysical Institute, University of Alaska Fairbanks, Fairbanks, Alaska

Peter A. Bieniek

International Arctic Research Center, University of Alaska Fairbanks, Fairbanks, Alaska

Received 6 December 2017; in final form 21 June 2018

ABSTRACT: Climate warming is expected to disproportionately affect crop yields in the southern United States due to excessive heat stress, while presenting new farming opportunities through a longer growing season farther north. Few studies have investigated the impact of this warming on agro-climate indices that link meteorological data with important field dates in northern regions. This study employs regional dynamical downscaling using the Weather

[a] Corresponding author: Rick Lader, rtladerjr@alaska.edu

DOI: 10.1175/EI-D-17-0036.1

Unauthenticated | Downloaded 12/28/22 08:07 PM UTC

Research and Forecasting (WRF) Model to assess changes in growing season length (GSL), spring planting dates, and occurrences of plant heat stress (PHS) for five regions in Alaska. Differences between future representative concentration pathway 8.5 (RCP8.5; 2011–40, 2041–70, 2071–2100) and historical (1981–2010) periods are obtained using boundary forcing from the Geophysical Fluid Dynamics Laboratory Climate Model, version 3, and the NCAR Community Climate System Model, version 4. The model output is bias corrected using ERA-Interim. Median GSL shows increases of 48–87 days by 2071–2100, with the largest changes in northern Alaska. Similarly, by 2071–2100, planting dates advance 2–4 weeks, and PHS days increase from near 0 to 5–10 instances per summer in the hottest areas. The largest GSL changes occur in the mid- (2041–70) and late century (2071–2100), when a warming signal emerges from the historical interannual variability. These periods coincide with the greatest divergence of the RCPs, suggesting that near-term decision-making may affect substantial future changes. Early-century (2011–40) projections show median GSL increases of 8–27 days, which is close to the historical standard deviation of GSL. Thus, internal variability will remain an important source of uncertainty into the midcentury, despite a trend for longer growing seasons.

KEYWORDS: Arctic; Climate prediction; Regional models; Agriculture

1. Introduction

1.1. Agronomic considerations in the context of warming

Climate change, largely influenced by anthropogenic emissions, is expected to disrupt agricultural production, globally and within the United States, due to changes in temperature, precipitation, and the resultant alterations to water availability (IPCC 2014). In 2016, over 800 million people globally were considered undernourished—an increase from the year before—and extreme drought and flooding were identified as key factors (FAO 2017). The anticipated global agronomic impacts of a warming climate suggest that higher atmospheric CO_2 will support plant fertilization through increased photosynthesis, but these benefits will be offset by greater plant heat stress and declining yields (Tripathi et al. 2016).

The effects of high temperatures on agriculture are particularly notable. In the contiguous United States (CONUS), Hsiang et al. (2017) found an average projected decrease of 9.1% in agricultural yield per 1°C of warming for maize, wheat, soybeans, and cotton; however, locations in the Northwest displayed increases greater than 30%. These findings represent average values, but excessive heat results in negative yield impacts that are nonlinear (Schlenker and Roberts 2009). Above a high temperature threshold, a plant must adapt by producing heat shock proteins that promote thermal tolerance; if the heat is too severe, the plant cells lose viability (Krishnan et al. 1989). Typical threshold values—expressed as daily mean temperature—for corn, rice, wheat, and grain legumes are 38°, 34°, 26°, and 25°C, respectively (Wahid et al. 2007). A warming climate will disproportionately affect agriculture in locations where these thresholds are exceeded, while the reduction of freezing temperatures will provide new opportunities to colder regions.

Amid increasing atmospheric CO_2 concentrations that now exceed 400 ppm (NOAA/ESRL 2017), no place in the United States is expected to warm at a greater rate than Alaska. The observed rate of warming in the Arctic is approximately

Unauthenticated | Downloaded 12/28/22 08:07 PM UTC

twice that of the global average (AMAP 2017), and the 12-month period from September 2015 to October 2016 was the warmest since records began in 1900 (Overland et al. 2016). Over mainland Alaska, 38% of the land is estimated to contain near-surface permafrost, and this is expected to reduce to 10%–18% by the end of the century, depending on emissions scenario; the greatest reductions are expected for the Seward Peninsula and Interior Alaska (Pastick et al. 2015). For land areas poleward of 45°N, growing season length increased 2.6 days decade^{-1} from 1982 to 2014, but substantial spatiotemporal variability was observed (Park et al. 2016).

1.2. Study area

Given its harsh climate, less than 0.5% of Alaska's land area comprises farmland; however, the total cropland in Alaska increased by 55%, or approximately 30 000 acres, from 1982 to 2012, with over one-quarter of this area for hay and green silage (USDA/NASS 2014a). The vast majority of this and the lesser-grown barley, oat, and wheat crops are located in the valley locations between Anchorage and Fairbanks (Figure 1a). These Interior valleys exhibit an extreme annual temperature cycle, often marking the coldest and hottest parts of Alaska with temperatures as low as −50°C in winter and up to 35°C during summer. Largely protected from extreme precipitation by surrounding mountains, these valleys receive adequate rainfall and long hours of solar radiation, conducive for plant growth. Outside of field crops in this zone, the state's remaining agricultural production is in berries, fruits, vegetables, and floriculture. Small-scale greenhouses are common in the shoulder seasons to extend activities. Most coastal areas are too cool, cloudy, and wet during the summer months for extensive production.

Rapid warming in Alaska could affect these historical conditions, and threshold-based agro-climate indices represent a way to link meteorological data with important field dates and thermal accumulation units. Matthews et al. (2008) codeveloped a set of indicators with stakeholders in Scotland's agriculture industry that include the start-of-field operations date, growing season length, first and last air frost, and plant heat stress. Regional climate model projections of these indices across the United Kingdom from 2061 to 2090 show an increased growing season length of approximately 2 months, with the largest changes occurring in the coldest locations (Harding et al. 2015). Applying these metrics to the CONUS, Monier et al. (2016) found an increased growing season length in excess of 3 months for parts of the Northwest and Northeast under the business-as-usual scenario (RCP8.5). It is also noted that mitigation of greenhouse gas emissions could greatly reduce the negative impacts of excessive heat, decreased water availability, and subsequent lower yields (Beach et al. 2015), although mitigation of emissions would also reduce the increase of growing season length.

The present study builds on this previous research and assesses projected agricultural opportunity for Alaska to 2100, producing a set of agro-climate variations using downscaled climate model simulations and reanalysis. These indices include 1) growing season length, defined as the difference in days between the last frost on or before 30 June and the first frost on or after 1 July; 2) start-of-field operations (SFO), which represents the calendar date when the thermal accumulation of daily

Unauthenticated | Downloaded 12/28/22 08:07 PM UTC

a)

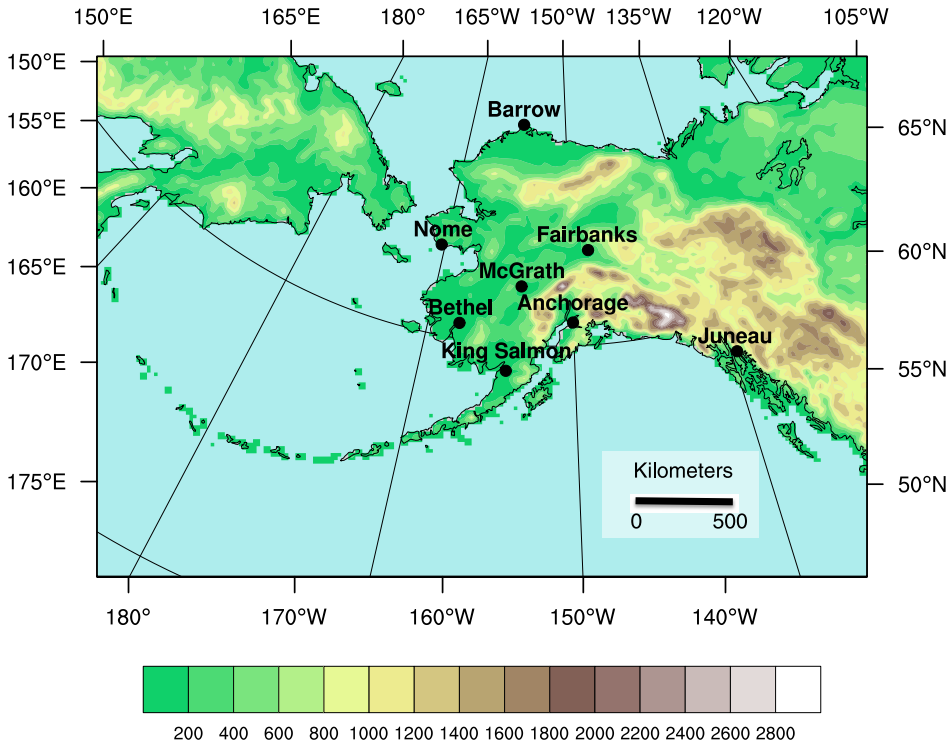

b)

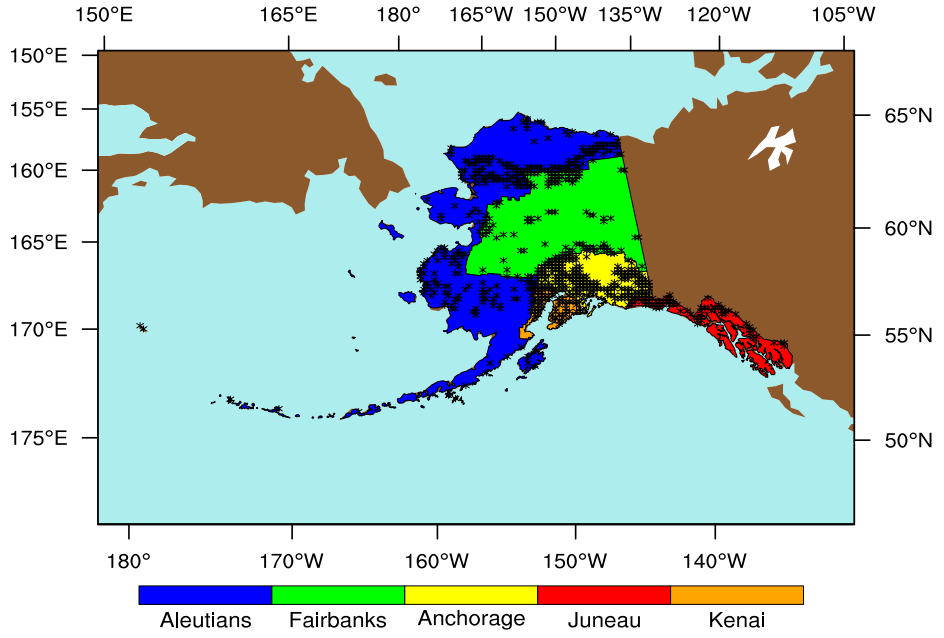

Figure 1. (a) Model terrain height (m) and (b) USDA Alaska census areas. Black hatching denotes nonsoil grid cells. The latitude and longitude coordinates for the cities are as follows: Anchorage (61.17°, 150.02°W), Barrow (71.30°N, 156.78°W), Bethel (60.78°N, 161.80°W), Fairbanks (64.80°N, 147.88°W), Juneau (58.30°N, 134.41°W), King Salmon (58.68°N, 156.65°W), McGrath (62.97°N, 155.62°W), and Nome (64.50°N, 165.43°W).

Unauthenticated | Downloaded 12/28/22 08:07 PM UTC

average temperature T_{avg} reaches 200°C; and 3) plant heat stress (PHS), defined as the number of days with a T_{avg} that exceeds 25°C. The resulting information on these metrics helps to inform the following questions:

1) How is Alaska's growing season length (GSL) projected to change this century, both spatially and in terms of differences between the last spring air frost (LF) and first autumn air frost (FF)?
2) Can the SFO index, derived from the downscaled data, be used as a proxy for planting date?

2. Data and methods

2.1. Observed growing season trends

The GSL in Alaska, defined as the period between the last air frost (hereafter frost; minimum temperature $T_{min} \leq 0$°C) in the first half of the year (i.e., no later than 30 June) and the first frost in the second half (i.e., on 1 July or later), ranges from over 5 months in the southeast to effectively zero from the Brooks Range northward. Trends were calculated via linear regression of the annual GSL time series of station observations [Menne et al. (2012); https://www.ncdc.noaa.gov/ghcn-daily-references], and statistical significance of the regression coefficients was tested using the two-tailed t test. Station observations during the historical period (1981–2010) show mixed, but primarily increasing, GSL trends that range from −9.1 days decade^{-1} at Juneau to 6.3 days decade^{-1} at Fairbanks (Figure 2). Both of these values are statistically significant at the 95% confidence level. The trend of GSL at Fairbanks compares well with results from a 100-yr record, beginning in 1906, which show a 45% increase in growing season (Wendler and Shulski 2009).

Over the longest available period of record for each station, GSL trends are generally 1–3 days decade^{-1} (Figure 2). These trends (in days decade^{-1}) are significant at the 95% confidence level at Anchorage (1.9), Barrow (now known as Utqiaġvik; 1.2), Bethel (2.7), Fairbanks (2.7), Juneau (3.4), and Nome (3.1). Only King Salmon (−2.0) shows a decreased GSL. These trends are smaller than for the historical period, but are in the same direction, with the exception of Juneau. The opposing rates of change at Juneau highlight an issue with calculating trends over short time intervals when outliers and the starting point used can exert a greater influence. The 10-yr running-mean results in Figure 2, presented to reduce noisiness for illustration, show that these trends are affected by high interannual and decadal variability. At Juneau, several of the longest growing seasons occurred in the mid-1980s, at the beginning of the historical period.

2.2. Downscaled reanalysis and climate model data

This study includes multiple regional dynamically downscaled variables obtained using the Advanced Research core of the Weather Research and Forecasting Model (WRF; Skamarock et al. 2008) over the Alaska domain (Figure 1a). The model simulations were driven by ERA-Interim (Dee et al. 2011) from 1981

Unauthenticated | Downloaded 12/28/22 08:07 PM UTC

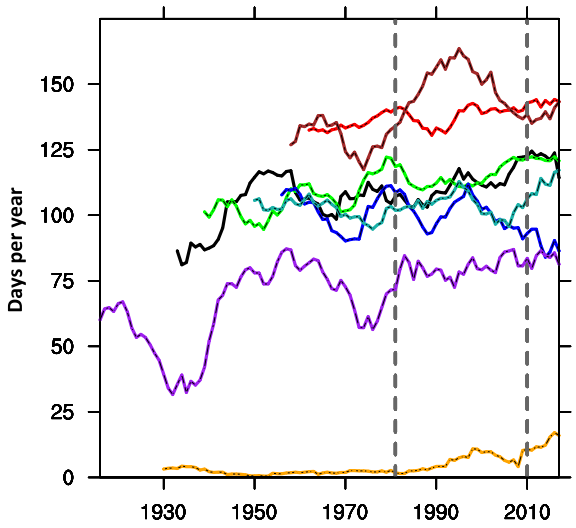

City	Full Period of Record	1981-2010
Anchorage	**1.9**	5.1
Barrow	**1.2**	4.4
Bethel	**2.7**	5.7
Fairbanks	**2.7**	**6.3**
Juneau	**3.4**	**-9.1**
King Salmon	-2.0	-2.1
McGrath	1.1	1.0
Nome	**3.1**	4.4

Figure 2. Observed 10-yr running mean of annual GSL for eight cities in Alaska. The points represent the last year of the 10-yr sliding window used for averaging (e.g., 1917 signifies 1908–17). Vertical dashed lines demarcate the historical period in this study (1981–2010). The linear trend (days decade^{-1}) is shown with significance at the 95% confidence level, indicated in boldface for both periods.

to 2010; the Geophysical Fluid Dynamics Laboratory Climate Model version 3 (GFDL-CM3; Donner et al. 2011) from 1981 to 2100; and the National Center for Atmospheric Research Community Climate System Model, version 4 (CCSM4), from 1981 to 2100. The future data come from the business-as-usual representative concentration pathway (RCP8.5; Riahi et al. 2011) of phase 5 of the Coupled Model Intercomparison Project (CMIP5; Taylor et al. 2012). Because of the sparseness of station observations in Alaska, the downscaled reanalysis data are considered as gridded observations; however, in situ information is used when available for comparison.

The downscaling produced gridded fields at 20-km spatial and hourly time resolution and was conducted in 2-day segments, each reinitialized to the driving reanalysis or model. In addition, spectral nudging constrained the simulations to the original forcing data. A complete description of the WRF configuration is included in Bieniek et al. (2016). A few of the key physics options used here include the microphysics (Morrison two-moment; Morrison et al. 2009), radiation (Rapid Radiative Transfer Model; Iacono et al. 2008), the Noah land surface

Unauthenticated | Downloaded 12/28/22 08:07 PM UTC

module, and coupling to a thermodynamic sea ice model (Zhang and Zhang 2001). Bieniek et al. (2016) show that the dynamical downscaling reduces temperature and precipitation bias across Alaska when compared to coarse forcing data, and this was particularly true for locations with significant topography.

2.3. Bias-correction methodology

The agro-climate analysis in this study utilizes the five operational census areas of the United States Department of Agriculture (USDA) to demonstrate the spatial variability that is characteristic of Alaska and to highlight regional differences with regard to projected changes. Additionally, a layer that separates soil and nonsoil is superimposed atop the census areas (Figure 1b). The geographic information for these regions is available from the National Agricultural Statistics Service (USDA/NASS 2014b) and the soil layer from the Natural Resources Conservation Service (Soil Survey Staff 2017). The nonsoil grid cells, which are either coastal or mountainous, are not included in any of the indices described by this research. Projected changes to the agro-climate indices are presented in 30-yr time intervals (i.e., 2011–40, 2041–70, and 2071–2100) from both the CCSM4 and GFDL-CM3. These changes have been bias corrected according to the observation-based ERA-Interim (1981–2010). ERA-Interim is among the top-performing reanalyses with regard to surface temperature and precipitation for Alaska, frequently exhibiting the lowest root-mean-square error (RMSE) relative to station observations (Lader et al. 2016).

The projections were bias corrected using quantile mapping or the delta method, depending on the variable. For GSL, LF, and FF, the historical climate model distribution (1981–2010) is sorted in ascending order and is subtracted from the corresponding sorted 30-yr future distribution at each grid cell. These differences are then added to the sorted ERA-Interim distribution (1981–2010). For example, the *n*th-longest growing season modeled by CCSM4 during 1981–2010 is subtracted from the *n*th-longest projected growing season by CCSM4 during 2011–40. This difference, exclusively according to the climate model (i.e., CCSM4), is then added to the *n*th-longest observed growing season from ERA-Interim. Since 30-yr time intervals are used, $n = 30$. All changes are relative to the 1981–2010 historical period. By applying this quantile-based bias correction to each point of the 30-yr distributions, changes to the mean and variability of GSL, LF, and FF are captured. This delineation between time periods also allows investigation into if and when the projected change signal dominates the interannual variability.

The 30-yr projected changes in the SFO and PHS indices are presented as distributional means. The same delta method (Hayhoe 2010) is applied as before to bias correct the climate model output, but rather than subtracting at all $n = 30$ points of the respective distributions, the 30-yr mean is used instead. For example, the 30-yr historical (1981–2010) mean SFO date from CCSM4 is subtracted from the 2011–40 mean CCSM4 SFO date and added to the ERA-Interim (1981–2010) mean SFO date at each grid cell. For all of the agro-climate indices, the resulting gridcell values are further aggregated and averaged by the aforementioned census areas (Figure 1b).

Unauthenticated | Downloaded 12/28/22 08:07 PM UTC

3. Results

3.1. Temperature and precipitation climatology and projections

The seasonal ERA-Interim average surface temperature climatology (Figure 3, left), derived from daily data, shows a north-to-south gradient for all periods except for summer, when the highest temperatures are found across Interior lowlands, such as the Yukon Flats and Tanana Valley. Late-century temperatures (2071–2100) are projected to warm by 8.1°, 4.9°, 5.2°, and 5.7°C for winter (DJF), spring (MAM), summer (JJA), and autumn (SON), respectively, according to the CCSM4 (Figure 3, center). Larger increases of 10.2°, 7.7°, 7.0°, and 7.7°C are projected for the GFDL-CM3 (Figure 3, right). The future results indicate that the largest changes occur during DJF when the coldest temperatures are found across the Interior; concurrently, Arctic waters adjacent to Alaska stay close to freezing. The average temperature across Alaska transitions from below to above freezing for MAM and SON.

The seasonal ERA-Interim total precipitation climatology (Figure 4, left), also derived from daily data, shows that MAM is the driest season, and JJA is the wettest for Alaska when convective precipitation occurs. In all seasons, total precipitation is projected to increase; the largest changes with respect to magnitude and percentage for CCSM4 occur in DJF, and they occur in SON for GFDL-CM3. The CCSM4 (Figure 4, center) shows increases that are approximately half of those depicted by the GFDL-CM3 (Figure 4, right). For CCSM4, the smallest percentage change (17.1%) is in SON, while for GFDL-CM3, the smallest increases are in MAM (34.8%). The smallest change in actual magnitude for both models is during MAM.

3.2. Growing season length projections for Alaska

The widespread observed increases in GSL are projected to continue, and the rate is expected to accelerate across Alaska. The late-century (2071–2100) median increase in CCSM4 ranges from 48 days for the Fairbanks census area up to 63 days for the Aleutian Islands. Increases driven by the warmer GFDL-CM3 range from 67 to 87 days for the same census areas (Table 1). The future (2071–2100) and historical (1981–2010) periods are separated by 90 years, meaning that the modeled increases yield approximate trends of 5–10 days decade^{-1}. The lower end of this range compares well with historical trends (days decade^{-1}) at Anchorage (5.1), Barrow (4.4), Bethel (5.7), Fairbanks (6.3), and Nome (4.4), but is considerably higher than those from the full period of record (Figure 2). The projected changes indicate that the shortest late-century growing season is outside (i.e., longer) the historical interquartile growing season range for all census areas (Figure 5). The GSL distributions, including the median value and the extremes, become successively longer with each 30-yr time period. However, despite these large GSL increases, the projected census area GSL minima continue to exhibit overlap with the historical distributions in the CCSM4 results.

Projections from CCSM4 for the early-century period (2011–40) show increases to median GSL, depending on census area, that range from 8 (Fairbanks) to 15 (Juneau) days when compared to the historical period (Table 1). Greater changes

Unauthenticated | Downloaded 12/28/22 08:07 PM UTC

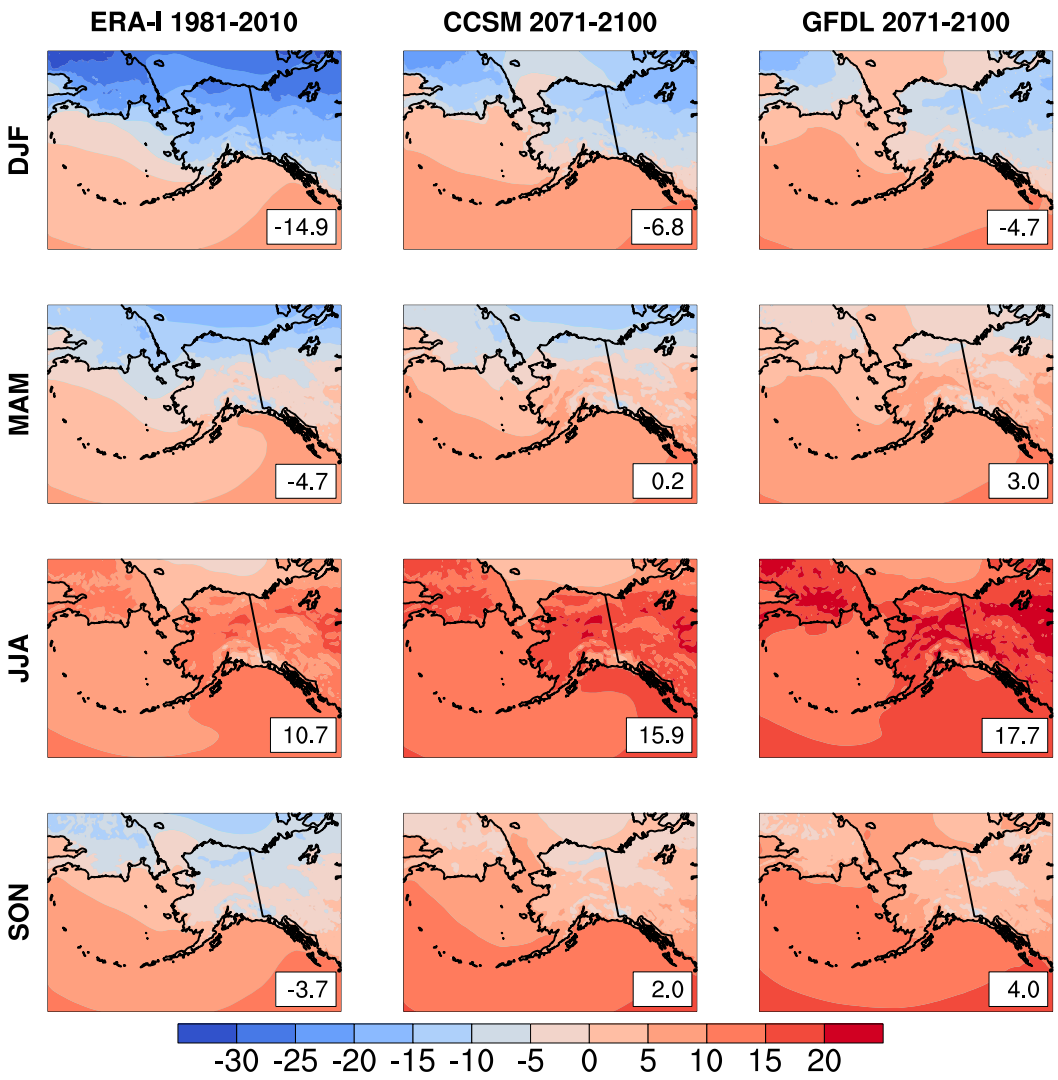

Figure 3. Seasonal 2-m temperature climatology (°C) from (left) ERA-Interim (1981–2010), (center) CCSM4 projected change (2071–2100 minus 1981–2010) added to ERA-Interim, and (right) GFDL-CM3 projected change (2071–2100 minus 1981–2010) added to ERA-Interim. The land gridcell average for Alaska is indicated in the bottom-right corner of each panel.

are found for the absolute minima and first quartile of the 30-yr distributions, but not necessarily for the third quartiles and maxima. For GFDL-CM3, median GSL increases from 17 (Juneau) to 27 (Aleutians) days. Similar to CCSM4, larger increases are found for the minima and first quartiles, while mixed results are shown for the upper points of the distributions. These changes have the effect of lowering the standard deviation of annual GSL for all census areas, according to CCSM4, and all regions except for the Juneau census area in GFDL-CM3.

For the midcentury period (2041–70), CCSM4 shows further median GSL increases, relative to the 2011–40 period, that vary between 18 (Fairbanks) and 23

Unauthenticated | Downloaded 12/28/22 08:07 PM UTC

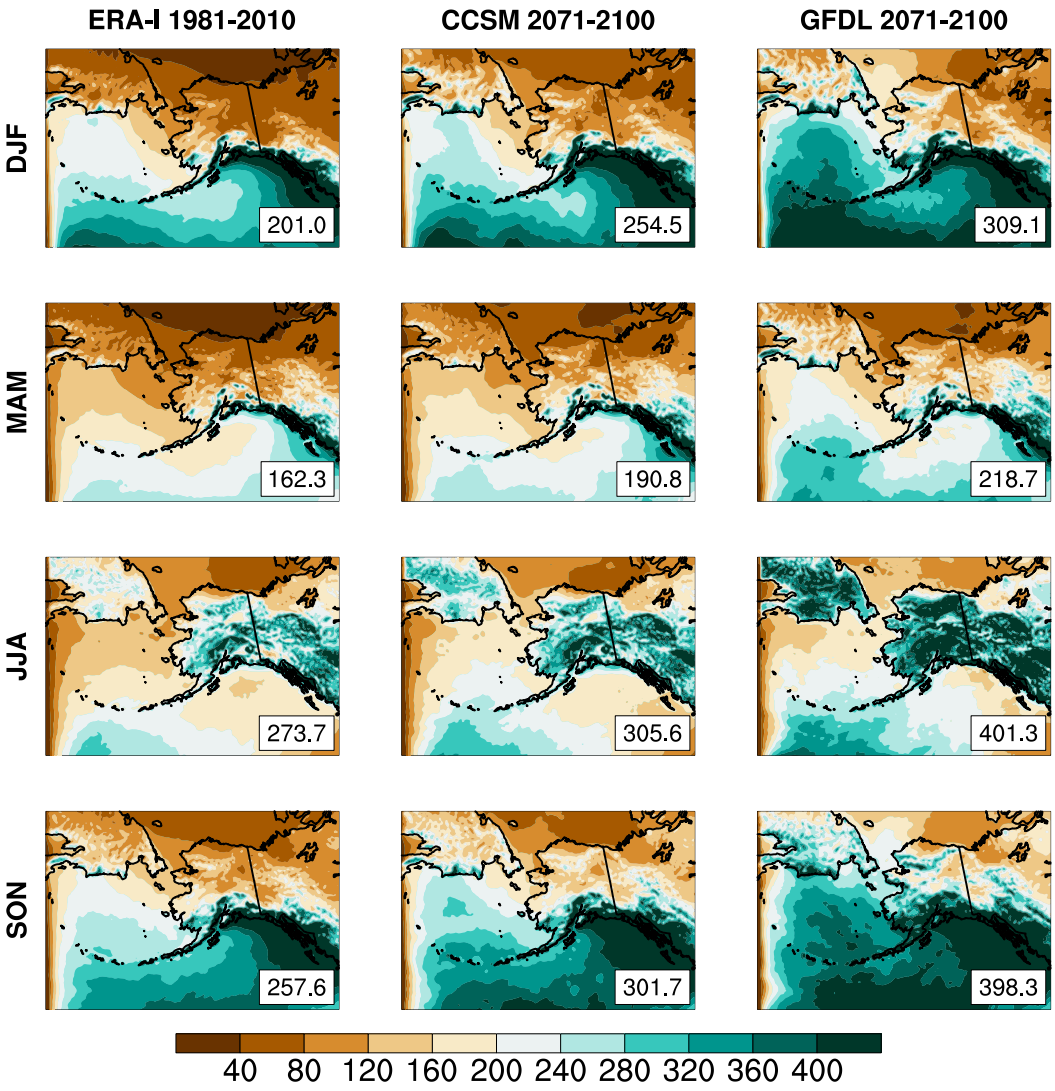

Figure 4. As in Figure 3, but for total seasonal precipitation (mm).

(Aleutians) days (Table 1). These increases are more pronounced for GFDL-CM3, which shows increases of 27–37 days for the Fairbanks and Anchorage census areas, respectively. One notable difference between the two models when comparing the midcentury with the early-century periods is their interannual variability. For CCSM4, each census area has a higher standard deviation of annual GSL from 2041–70 than during the 2011–40 period; the opposite is true for GFDL-CM3. This is reflected visually in Figure 5 by comparing the changes between the red and green box-and-whisker diagrams.

The late-century period (2071–2100) shows the greatest GSL increases for CCSM4, ranging from 19 to 27 days longer than the midcentury period for the Juneau and Aleutian Islands census areas, respectively; the range of increases according to GFDL-CM3 is comparable at 18–27 days for the Fairbanks and Aleutian Islands

Unauthenticated | Downloaded 12/28/22 08:07 PM UTC

Table 1. Minimum (Min), lower quartile (Q1), median (Med), upper quartile (Q3), and maximum (Max) GSL (days) averaged over USDA census areas for ERA-Interim (1981–2010) and bias-corrected scenarios for CCSM4 and GFDL-CM3. The greatest relative changes from successive periods for each census area and statistical point are indicated with the ending period in boldface.

		CCSM4					GFDL-CM3				
Area	Period	Min	Q1	Med	Q3	Max	Min	Q1	Med	Q3	Max
Aleutians	1981–2010	59	88	101	114	141	59	88	101	114	141
	2011–40	80	103	114	127	153	90	114	128	139	158
	2041–70	84	117	137	**153**	**181**	**129**	**151**	**161**	**170**	183
	2071–2100	**124**	**153**	**164**	175	198	157	177	188	198	**217**
Anchorage	1981–2010	57	87	99	110	133	57	87	99	110	133
	2011–40	71	101	112	123	150	**97**	117	125	**137**	157
	2041–70	81	118	133	**146**	171	134	**154**	**162**	170	181
	2071–2100	**123**	**151**	**160**	169	**195**	162	178	185	194	**209**
Fairbanks	1981–2010	77	104	118	129	150	77	104	118	129	150
	2011–40	91	115	126	137	152	105	128	140	151	168
	2041–70	102	130	144	**156**	**168**	**141**	**157**	**167**	**177**	**189**
	2071–2100	**138**	**155**	**166**	174	183	158	175	185	194	207
Juneau	1981–2010	140	165	176	188	213	140	165	176	188	213
	2011–40	**171**	181	191	204	236	160	182	193	206	245
	2041–70	184	199	210	222	264	**194**	**213**	**223**	**236**	261
	2071–2100	205	**219**	**229**	**244**	**303**	211	235	246	265	**300**
Kenai	1981–2010	104	132	142	151	176	104	132	142	151	176
	2011–40	131	146	154	163	**197**	**140**	153	163	172	196
	2041–70	138	162	174	186	214	167	**183**	**191**	197	218
	2071–2100	**169**	**185**	**195**	**206**	234	186	204	214	**224**	**254**

census areas, respectively (Table 1). The projected variability of GSL for Alaska again shows considerable spatial variations. Relative to the historical period, both models indicate a decreased late-century standard deviation of up to 1 week across much of the Interior and increases of up to 1 week from 60°N and points southward (Figure 6). The CCSM4 shows increases in variability (standard deviation) of up to 10 days along parts of the North Slope (Figure 6, top), while the GFDL-CM3 has decreased GSL variability exceeding 10 days for a large swath of this area (Figure 6, bottom). This is likely due to differences in the model sea ice state. From 2071 to 2100, the GFDL-CM3 shows essentially no sea ice in the study domain, producing more of a maritime climate for Arctic Alaska; however, the CCSM4 depicts high interannual sea ice variability during this period. These differences are evident in the GSL boxplots for the Aleutian Islands census area in Figure 5.

Analysis of the components that determine GSL, namely, the LF (Figure 7) and the FF (Figure 8), demonstrates that with each successive 30-yr period, the median date of LF is earlier, and the median date of FF is later. For CCSM4, the relative advances to median LF by census area range from 1 to 7 (2011–40), 10 to 13 (2041–70), and 8 to 12 (2071–2100) days when compared to the preceding 30-yr period. For GFDL-CM3, these values are generally larger: from 9 to 12 (2011–40), 12 to 19 (2041–70), and 7 to 14 (2071–2100) days (Table 2). The relative delays to median FF by census area range from 6 to 10 (2011–40), 4 to 11 (2041–70), and 8 to 12 (2071–2100) days for CCSM4 and from 8 to 17 (2011–40), 4 to 20 (2041–70), and 10 to 17 (2071–2100) days for GFDL-CM3 (Table 3).

Unauthenticated | Downloaded 12/28/22 08:07 PM UTC

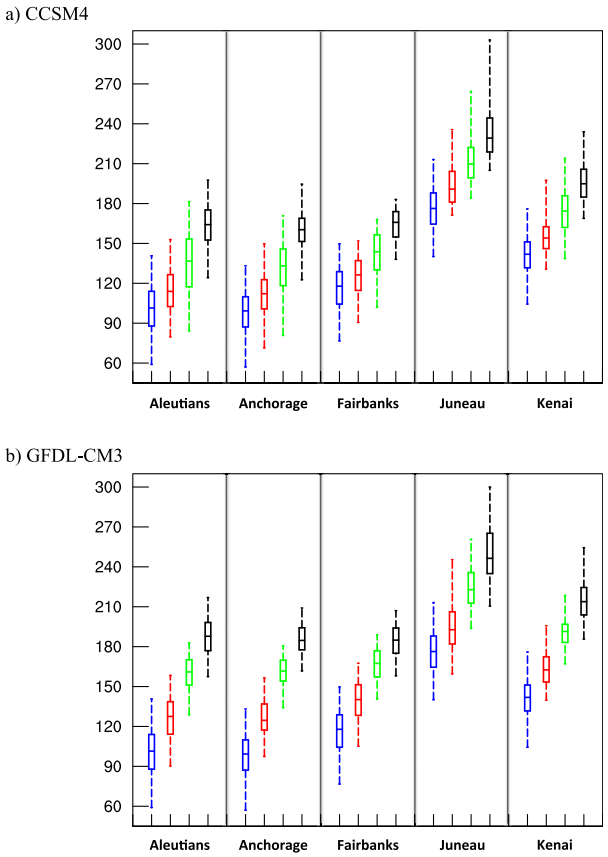

Figure 5. GSL (days year^{-1}) across five USDA census areas for (a) CCSM4 and (b) GFDL-CM3. Boxes represent the interquartile range, and whiskers show the extremes. Projected change, relative to model climatology, for 2011–40 (red), 2041–70 (green), and 2071–2100 (black) has been bias corrected with ERA-Interim (1981–2010; blue).

When comparing the late-century period (2071–2100) with the historical reference period (1981–2010), there is a tendency for larger changes to occur with the FF, indicating that the lengthening GSL is due more to later autumn frost than to earlier spring thaws. The primary exception to this is for the Juneau census area, where the change in the LF is about 1 week greater (i.e., earlier) than the change to later FF. It is speculated that the dearth of late-century snow cover in this southern region is the main reason for this difference. Much of the solar energy in the spring currently goes into melting snow and is projected to continue to do so to a lesser extent in northern regions, but not in the south. The late-century (2071–2100) CCSM4 shows an earlier date of LF, compared to the historical period, ranging from an advance of 19 (Fairbanks) to 31 (Juneau) days. For FF, the geographical range of values is larger: 23 (Juneau) to 40 (Aleutians) days later. The analogous ranges from the GFDL-CM3 for LF are 30 (Fairbanks) to 45 (Anchorage) days earlier than historical and 31 (Juneau) to 53 (Aleutians) days later for FF.

Unauthenticated | Downloaded 12/28/22 08:07 PM UTC

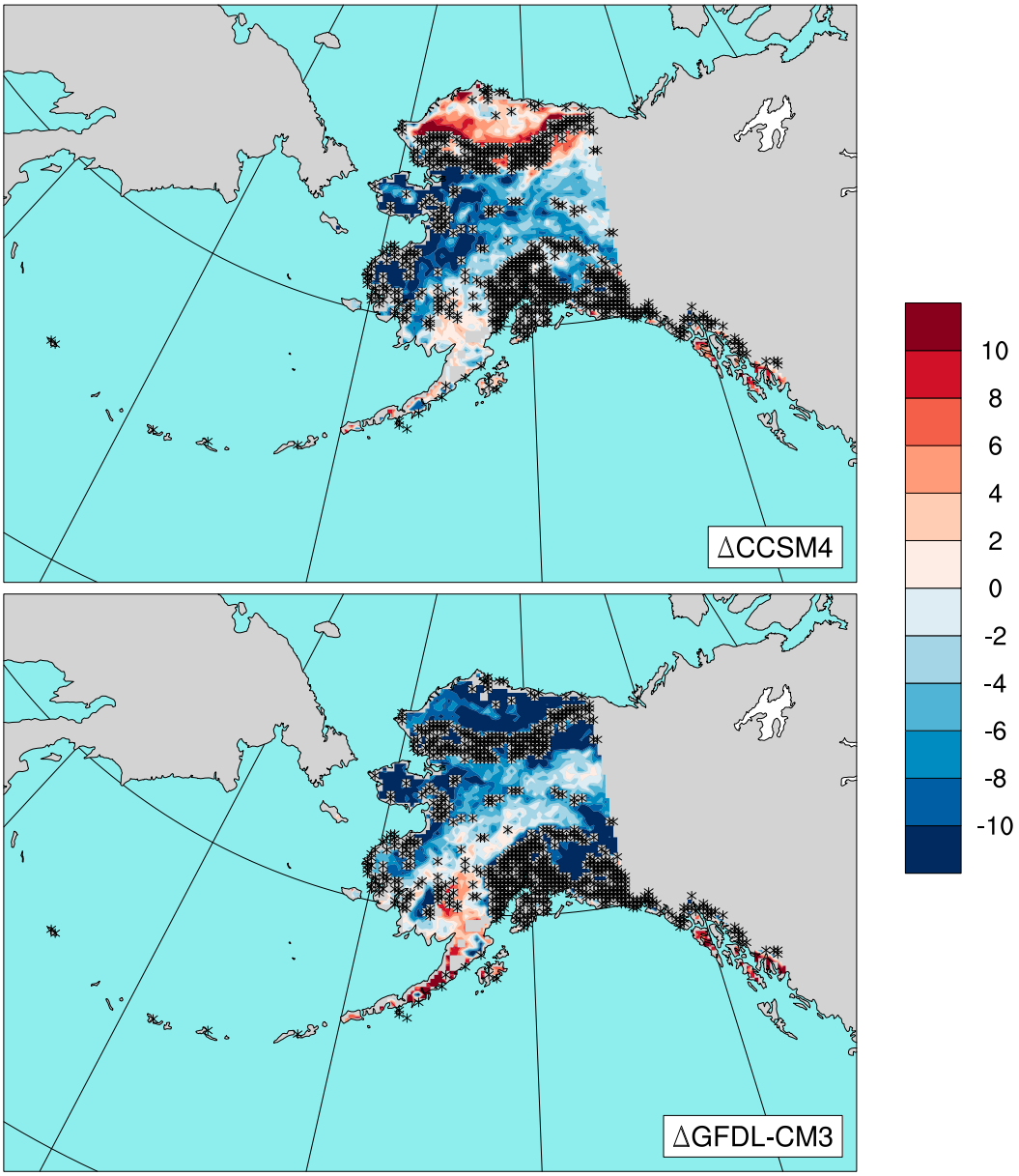

Figure 6. Projected changes (2071–2100), relative to climatology (1981–2010), of detrended standard deviation of GSL (days) for (top) CCSM4 and (bottom) GFDL-CM3. Black hatching denotes nonsoil grid cells. The latitude and longitude are identical to Figure 1.

3.3. Start-of-field operations date

A more robust measure for the start of the agricultural season than the last spring frost is the SFO index, which represents the date when the thermal accumulation (beginning 1 January) of daily T_{avg} reaches 200°C. When compared to the visually

Unauthenticated | Downloaded 12/28/22 08:07 PM UTC

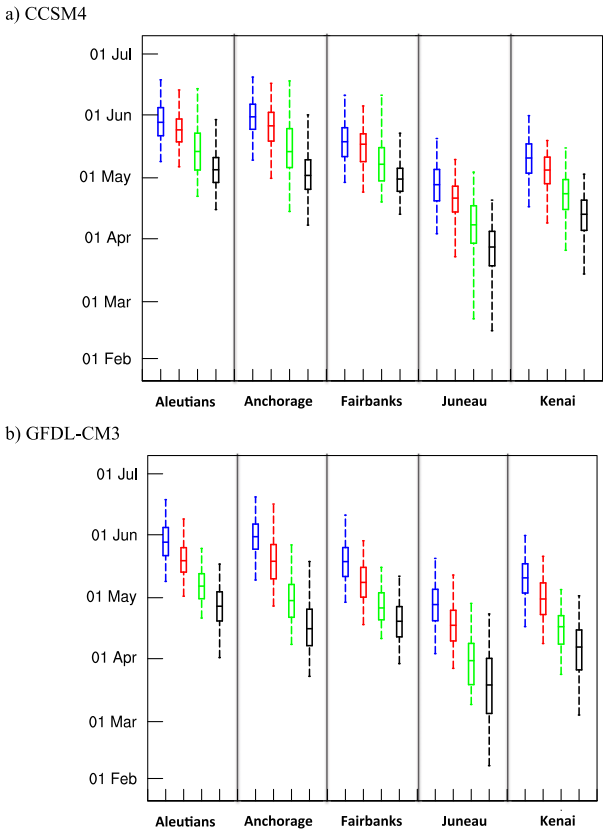

Figure 7. As in Figure 5, but for average last date of spring frost.

observed ‘‘green up’’ time series at Fairbanks (Figure 9), the independent time series of SFO derived from Fairbanks International Airport data and the nearest ERA-Interim grid cell have correlation coefficients of 0.91 and 0.90, respectively. Green-up refers to the period when deciduous plants leaf out in the spring. The photoperiod characteristic of Interior Alaska during the spring allows this change to occur over the course of 1 day, and it is striking to the visual observer as the landscape hue transitions from brown to green. Fathauer (2012) notes a concurrent relationship between green-up and grass pollen release. Because of its phenological importance, the onset of green-up in the Interior was statistically tested with daily maximum temperature as the primary predictor (Thoman and Fathauer 1998).

With the assumption that this temperature–green-up relationship can be extrapolated beyond Fairbanks, historical SFO dates range from late April over Southeast Alaska to late May across most of the Interior to late June for the North Slope. The CCSM4 projects earlier SFO dates, with changes ranging from less than 1 week (2011–40) to 1–2 weeks (2041–70) to about 2–4 weeks across Alaska (2071–2100; Figures 10a–c), while GFDL-CM3 shows earlier start dates of 1 week, 2 weeks, and approximately 1 month, respectively (Figures 10d–f).

Unauthenticated | Downloaded 12/28/22 08:07 PM UTC

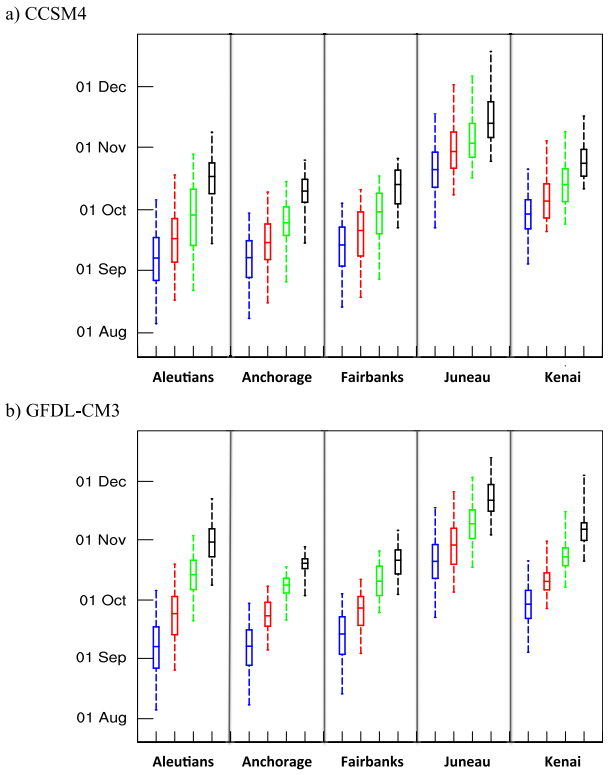

Figure 8. As in Figure 5, but for average first date of autumn frost.

3.4. Plant heat stress

Higher precipitation and a longer growing season are conducive to greater agricultural opportunity, but warmer temperatures pose a risk of increased PHS. Exposure to extremely high daily maximum temperature (e.g., >35°C) disrupts the carbon cycle in plants by reducing photosynthesis and increasing respiration (Barnabás et al. 2008). Wheat, a primary field crop currently grown in Alaska, shows cell deterioration with maximum temperatures above 25°C, and anthesis (i.e., flowering) is stunted above 32°C (Sánchez et al. 2014). Excessive heat causes plants to use energy to mitigate structural damage, and this lost energy can no longer be used for growth.

Following the results of Wahid et al. (2007), a typical metric used to indicate PHS for cool season crops that are common to Alaska is the number of days with T_{avg} greater than 25°C. Using T_{avg} instead of daily maximum temperature means that the plants have sustained prolonged exposure to high temperatures. No location in Alaska currently averages one PHS day per year (figure not shown); however, Alaska's Interior occasionally experiences this level of heat during a hot summer. Future projections indicate an increased number of heat stress days per year in the Interior and an introduction of such days to places that previously had none. The CCSM4 shows greater increases (Figures 11a–c), compared to the

Unauthenticated | Downloaded 12/28/22 08:07 PM UTC

Table 2. As in Table 1, but for date of last spring frost (Julian day).

		CCSM4					GFDL-CM3				
Area	Period	Min	Q1	Med	Q3	Max	Min	Q1	Med	Q3	Max
Aleutians	1981–2010	128	141	147	155	168	128	141	147	155	168
	2011–40	125	138	144	149	163	121	133	138	145	159
	2041–70	**111**	**124**	**133**	142	164	110	**120**	**126**	**132**	**144**
	2071–2100	104	118	124	**130**	**149**	**91**	109	116	123	137
Anchorage	1981–2010	129	144	150	156	170	129	144	150	156	170
	2011–40	120	138	146	152	167	116	129	138	146	166
	2041–70	**103**	**125**	**133**	144	168	**97**	**110**	**119**	**127**	**146**
	2071–2100	97	114	121	**129**	**151**	81	96	105	114	138
Fairbanks	1981–2010	118	130	138	145	161	118	130	138	145	161
	2011–40	113	128	137	142	155	107	120	128	135	148
	2041–70	108	**118**	**127**	135	161	100	**109**	**115**	**122**	**135**
	2071–2100	**102**	113	119	**125**	**142**	**88**	101	108	116	131
Juneau	1981–2010	92	109	117	124	139	92	109	117	124	139
	2011–40	81	103	110	116	129	85	99	106	114	131
	2041–70	**51**	**88**	**97**	106	123	67	**77**	**89**	**98**	**117**
	2071–2100	45	77	86	**94**	**109**	**37**	63	77	90	112
Kenai	1981–2010	106	122	130	137	151	106	122	130	137	151
	2011–40	98	117	124	130	138	97	112	119	127	140
	2041–70	**84**	**104**	**112**	**119**	135	82	**97**	**106**	**111**	**124**
	2071–2100	73	94	102	109	**122**	**62**	84	96	104	121

GFDL-CM3 (Figures 11d–f), with maximum frequencies exceeding 7 days yr^{-1} in parts of the Yukon Flats and Tanana Valley by 2071–2100. Each 30-yr projected period shows a slight increase in PHS days, compared to the previous 30 years.

Table 3. As in Table 1, but for date of first autumn frost (Julian day).

		CCSM4					GFDL-CM3				
Area	Period	Min	Q1	Med	Q3	Max	Min	Q1	Med	Q3	Max
Aleutians	1981–2010	217	238	249	259	278	217	238	249	259	278
	2011–40	228	247	259	269	**290**	**237**	**255**	266	275	291
	2041–70	233	255	270	**283**	301	262	278	**286**	**293**	306
	2071–2100	**256**	**281**	**289**	296	311	281	295	303	310	**325**
Anchorage	1981–2010	219	239	249	258	271	219	239	249	258	271
	2011–40	227	248	257	266	282	**247**	**260**	**265**	**272**	280
	2041–70	237	260	267	274	287	263	277	281	284	290
	2071–2100	**257**	**277**	**282**	**288**	**298**	275	289	292	294	**300**
Fairbanks	1981–2010	225	245	256	264	276	225	245	256	264	276
	2011–40	230	250	263	272	283	246	260	269	275	284
	2041–70	239	261	272	281	290	**267**	**275**	**283**	**290**	**298**
	2071–2100	**264**	**276**	**286**	**293**	**298**	276	286	293	299	309
Juneau	1981–2010	264	284	293	302	320	264	284	293	302	320
	2011–40	**280**	294	302	312	335	277	291	301	310	329
	2041–70	289	299	306	316	339	290	305	312	319	336
	2071–2100	297	**309**	**316**	**327**	**351**	**307**	**319**	**324**	**332**	**346**
Kenai	1981–2010	246	264	271	278	293	246	264	271	278	293
	2011–40	262	269	277	286	**307**	**269**	**278**	283	287	303
	2041–70	266	277	286	293	312	280	291	295	300	318
	2071–2100	**283**	**290**	**296**	**303**	319	293	304	**309**	**313**	**337**

Unauthenticated | Downloaded 12/28/22 08:07 PM UTC

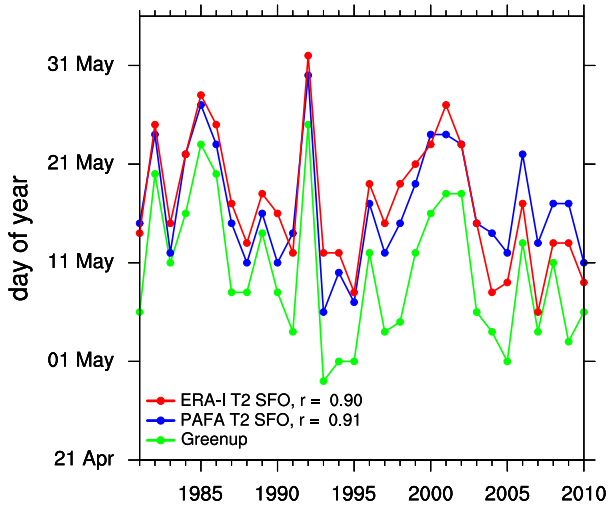

Figure 9. Annual time series (1981–2010) of visually observed green-up date (green), SFO date for Fairbanks International Airport (blue), and the SFO for the nearest grid cell from the downscaled ERA-Interim (red). The correlation coefficient *r* of each SFO time series compared to green-up is indicated.

4. Discussion

This study depicts changes in 30-yr segments beyond the historical period of 1981–2010 to allow for a climate change signal to emerge from the natural variability. Table 1 identifies the greatest relative GSL changes from successive periods in boldface for each of the 5 census areas and for each of the 5 statistical points, for a total of 25 per model. By adding these instances together and binning them into each of the three projected periods, it is found that the greatest GSL changes according to CCSM4 occur in the late-century period and in the midcentury for the GFDL-CM3. Similarly, for LF (Table 2), the greatest changes occur in the midcentury period for both models, and none of the highest relative changes occur in the early century (2011–40). For FF (Table 3), both models indicate that the greatest changes occur during the late century.

The relative increases in median GSL from the historical period to the early century are comparable to the historical standard deviation of GSL, meaning that internal variability will continue to be as important as the underlying trend into the midcentury. However, the signal of increased GSL largely emerges in all five census areas (Figure 5), such that most late-century growing seasons (2071–2100) will be reliably longer than currently observed, even in a relatively cold year. This is important for long-term planning, but highlights an ongoing problem. That is, despite rapid warming in the high latitudes, the economic risk of a failed crop due to a cold summer is an impediment to changing agricultural practices. The RCP8.5 emissions scenario used in this study shows the current trajectory of agroclimate indices for Alaska, but mitigation efforts could result in smaller observed changes.

Unauthenticated | Downloaded 12/28/22 08:07 PM UTC

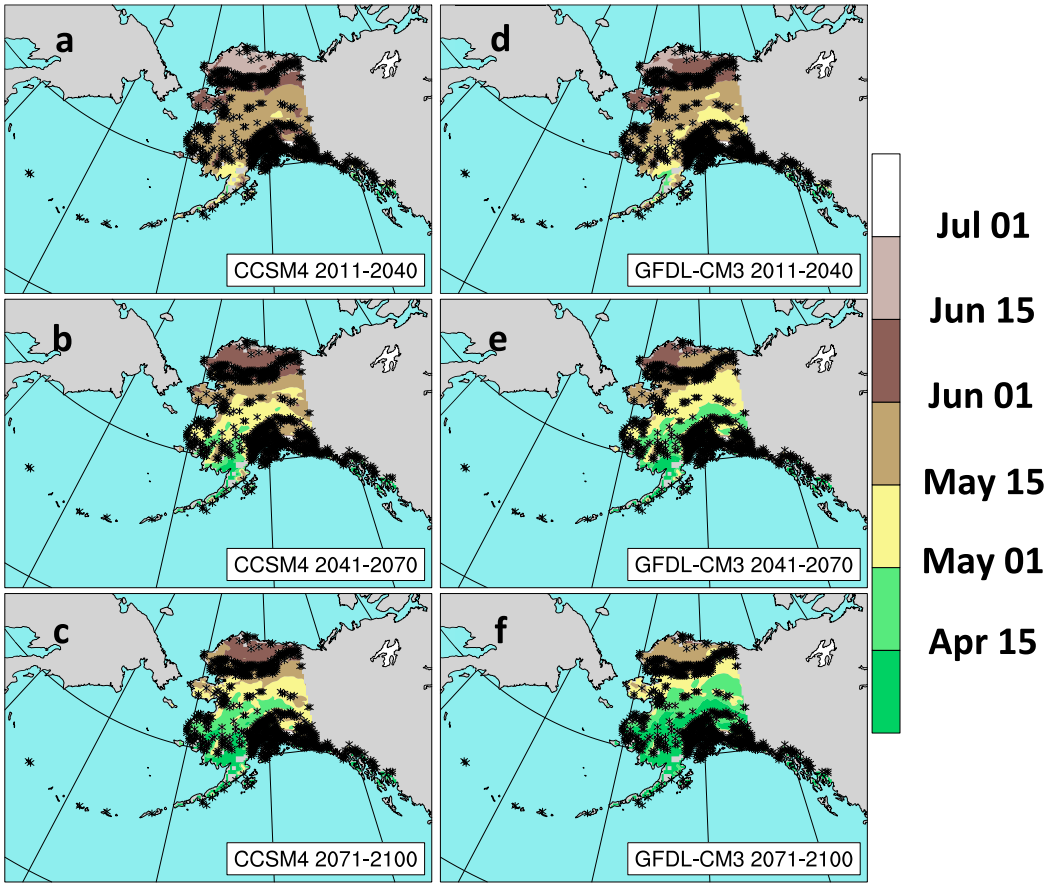

Figure 10. Average SFO date for (a)–(c) CCSM4 and (d)–(f) GFDL-CM3 by 30-yr period. Modeled change has been bias corrected with ERA-Interim (1981–2010). Black hatching denotes nonsoil grid cells. The latitude and longitude are identical to Figure 1.

Field sites near Fairbanks show a close relationship between planting date and green-up. The average planting date from 1978 to 2002 was 10 May (Van Veldhuizen and Knight 2004), and the average green-up date from 1981 to 2010 was 9 May (Figure 9). The average last frost at Fairbanks from 1978 to 2002 was 16 May (NOAA/NWS 2017), which coincides with the average SFO date from the Fairbanks International Airport and the nearest downscaled ERA-Interim grid cell (Figure 9). Given the statistically significant correlation between green-up and the SFO, these findings imply that the model output can provide a proxy for planting date. Heat accumulation metrics are commonly used to anticipate plant growth and maturation, usually measured in growing degree-days (GDD; Miller et al. 2001); the SFO uses heat units to estimate when the planting process can begin.

This study delineated soil versus nonsoil areas. A defining characteristic for much of the soil in Alaska is the presence of permafrost beneath the surface, which drains poorly and is classified by the gelisol taxonomic order (Soil Survey Staff

Unauthenticated | Downloaded 12/28/22 08:07 PM UTC

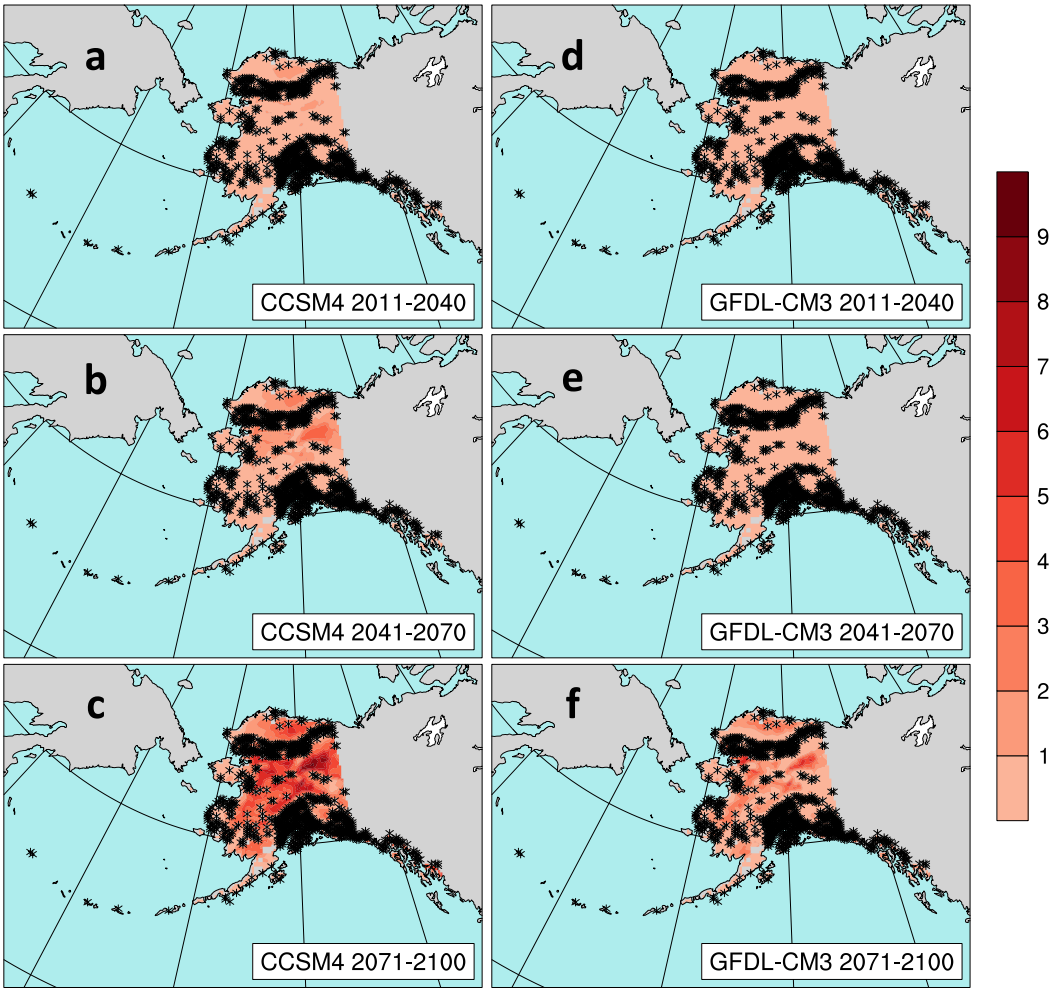

Figure 11. As in Figure 10, but for number of PHS days per year (T_{avg} > 25°C).

2014). Given the observed and projected rates of warming for Alaska, near-surface permafrost is expected to thaw over much of mainland Alaska. Thawing permafrost facilitates drainage of surface water, but in a climatologically dry area like mainland Alaska, the amount of soil water necessary for farming is a delicate balance that can rapidly transition from saturated to too dry. Thawing permafrost often leads to irregular subsidence and irregular surfaces (gullies and ridges) known as thermokarst, especially where the near-surface layers have high ice content. In such cases, extreme surface roughness can preclude agriculture. Furthermore, while the dynamically downscaled data used here provide a better representation of temperature and precipitation than the coarser forcing data (Bieniek et al. 2016; Lader et al. 2017), the 20-km resolution does not resolve the landscape at the individual field level. The feasibility of particular crop varieties can vary widely with small changes in elevation and prevailing meteorological quantities (Van Veldhuizen and Knight 2004).

Unauthenticated | Downloaded 12/28/22 08:07 PM UTC

One potential indicator of the changing feasibility of agriculture is the prevalence of biomass. While summer warming has been linked to higher biomass across the Arctic, several locations in Alaska have shown decreases in recent decades, pointing to a role of internal variability in complicating a warming climate. For example, southwest Alaska saw a reduction of biomass (i.e., browning) from 1982 to 2011 (Bhatt et al. 2013). Later spring snowmelt that delayed green-up has been suggested as a plausible reason for this finding (Bieniek et al. 2015). This is consistent with a pan-Arctic study of snow showing that while the region has decreasing snow-cover duration and snow water equivalent (SWE) in general, southwest Alaska represents one area with increased SWE and later snowmelt dates from 1979 to 2009 (Liston and Hiemstra 2011). Conversely, increased winter snow acts to insulate the soil underneath, keeping it warmer and more vulnerable to thawing in the summer. Surface water from permafrost thawing reduces the remotely sensed normalized difference vegetation index (NDVI), which is sensitive to soil moisture and water, thus potentially leading trends suggesting vegetation browning (Raynolds and Walker 2016). Parent and Verbyla (2010) suggest that an area of vegetation browning in eastern Interior Alaska resulted from drought stress and insect infestation, which, together with warming temperatures and thawing permafrost, overwhelmed any precipitation changes.

Greater agricultural opportunity has been noted for other high-latitude regions, but with a few causes for concern. Winter and spring wheat yields are projected to increase by an average of 37% and 70%, respectively, across western Canada from 2040 to 2069, but there are concerns about pests and new diseases (Smith et al. 2013). The potential for longer growing seasons has been recognized in Sweden and Finland, although the integration of transformational practices such as changing land usage for farming has been limited by short-term economic and regulatory concerns (Juhola et al. 2017). Uncertainty about changes in water stress at northern locations remains high, too. While precipitation is projected to increase, higher temperatures and longer summers will increase evapotranspiration. However, there is evidence that higher CO_2 will decrease stomatal conductance in plants, helping them to retain water (Yu et al. 2004).

5. Conclusions

This study investigates projected changes (2011–40, 2041–70, and 2071–2100) to agro-climate indices for Alaska using downscaled regional climate model simulations under the RCP8.5 emissions scenario, together with observed meteorological and reanalysis data. The average GSL is projected to increase by 48–87 days yr^{-1} when comparing the late century (2071–2100) with the historical reference period (1981–2010), with the largest changes in the coldest locations. Most areas exhibit more change to the first autumn frost than to the last spring frost. Southern Alaska is the exception to this, which could implicate the lack of seasonal snowpack here at the end of winter. The heat-unit-based SFO index exhibits a significant correlation with the independently observed green-up date at Fairbanks, which is subsequently related to observed planting date. These relationships indicate, by means of projections of the SFO across Alaska, the feasibility of earlier spring cultivation by 2–4 weeks. Increasing heat is also expected to result in greater PHS for field crops. Interior sites rarely have days with $T_{avg} > 25°C$ at present, but

Unauthenticated | Downloaded 12/28/22 08:07 PM UTC

these events are anticipated to occur 5–10 times per year in the hottest valleys at the end of this century.

The most pronounced GSL changes are projected to occur in the mid- and late-century periods, which also coincides with when the RCPs diverge the most (Kunreuther et al. 2014) and when the choice of scenario represents the highest source of uncertainty, compared to model spread and internal variability (Hodson et al. 2013). Utilizing a forcing scenario lower than RCP8.5 would reduce the anticipated late-century increases to temperature and precipitation. This would subsequently reduce the GSL, changes to the SFO, and PHS, while acting to preserve the current landscape of Alaska. Without land-use alterations and transformational changes to infrastructure, water management, and soil treatment, it is plausible that much of Alaska will remain untilled, despite the more favorable climate described here. However, the projections indicate far fewer days with freezing temperatures in Alaska. Thus, plants will be less susceptible to lethal cold temperatures, allowing for both an expansion in the acreage of crops that are currently grown and the introduction of new crops (e.g., maize) that require more growing degree-days. Additional investigation into the changing soil water balance and other effects of permafrost thaw would greatly improve further agriculture feasibility studies for Alaska.

Acknowledgments. We thank two anonymous reviewers who provided invaluable recommendations to help improve this manuscript. Support for this work was provided by the National Science Foundation, Office of Polar Programs through Grant PLR-1268350 and by the NOAA Climate Program Office through Grant NA16OAR4310162 to the Alaska Center for Climate Assessment and Policy. The project described in this publication was supported by Cooperative Agreements G10AC00588 and G17AC00213 from the United States Geological Survey. Its contents are solely the responsibility of the authors and do not necessarily represent the views of the Alaska Climate Adaptation Science Center or the USGS. This manuscript is submitted for publication with the understanding that the United States Government is authorized to reproduce and distribute reprints for governmental purposes. This work was supported in part by the high-performance computing and data storage resources operated by the Research Computing Systems Group at the University of Alaska Fairbanks, Geophysical Institute. Rick Thoman of the National Weather Service Alaska Region provided the historical green-up dates used in this study.

References

AMAP, 2017: Snow, water, ice and permafrost in the Arctic: Summary for policy-makers. Arctic Monitoring and Assessment Programme Rep., 20 pp., https://www.amap.no/documents/doc/snow-water-ice-and-permafrost.-summary-for-policy-makers/1532.

Barnabás, B., K. Jäger, and A. Fehér, 2008: The effect of drought and heat stress on reproductive processes in cereals. *Plant Cell Environ.*, **31**, 11–38, https://doi.org/10.1111/j.1365-3040.2007.01727.x.

Beach, R. H., and Coauthors, 2015: Climate change impacts on US agriculture and forestry: Benefits of global climate stabilization. *Environ. Res. Lett.*, **10**, 095004, https://doi.org/10.1088/1748-9326/10/9/095004.

Bhatt, U. S., and Coauthors, 2013: Recent declines in warming and vegetation greening trends over pan-Arctic tundra. *Remote Sens.*, **5**, 4229–4254, https://doi.org/10.3390/rs5094229.

Unauthenticated | Downloaded 12/28/22 08:07 PM UTC

Bieniek, P. A., and Coauthors, 2015: Climate drivers linked to changing seasonality of Alaska coastal tundra vegetation productivity. *Earth Interact.*, **19**, https://doi.org/10.1175/EI-D-15-0013.1.

——, U. S. Bhatt, J. E. Walsh, T. S. Rupp, J. Zhang, J. R. Krieger, and R. Lader, 2016: Dynamical downscaling of ERA-Interim temperature and precipitation for Alaska. *J. Appl. Meteor. Climatol.*, **55**, 635–654, https://doi.org/10.1175/JAMC-D-15-0153.1.

Dee, D. P., and Coauthors, 2011: The ERA-Interim reanalysis: Configuration and performance of the data assimilation system. *Quart. J. Roy. Meteor. Soc.*, **137**, 553–597, https://doi.org/10.1002/qj.828.

Donner, L. J., and Coauthors, 2011: The dynamical core, physical parameterizations, and basic simulation characteristics of the atmospheric component AM3 of the GFDL global coupled model CM3. *J. Climate*, **24**, 3484–3519, https://doi.org/10.1175/2011JCLI3955.1.

FAO, 2017: The state of food security and nutrition in the world 2017: Building resilience for peace and food security. FAO, IFAD, UNICEF, WFP, and WHO Rep., 132 pp., http://www.fao.org/3/a-I7695e.pdf.

Fathauer, T., 2012: The relation of spring pollen release to weather in Fairbanks, Alaska. M.S. thesis, Dept. of Atmospheric Sciences, University of Alaska at Fairbanks, 85 pp., http://ffden-2.phys.uaf.edu/atm/atm/theses/Fathauer_Ted_MS2012.pdf.

Harding, A. E., M. Rivington, M. J. Mineter, and S. F. B. Tett, 2015: Agro-meteorological indices and climate model uncertainty over the UK. *Climatic Change*, **128**, 113–126, https://doi.org/10.1007/s10584-014-1296-8.

Hayhoe, K. A., 2010: A standardized framework for evaluating the skill of regional climate downscaling techniques. Ph.D. dissertation, University of Illinois at Urbana–Champaign, 158 pp., https://www.ideals.illinois.edu/handle/2142/16044.

Hodson, D. L. R., S. P. E. Keeley, A. West, J. Ridley, E. Hawkins, and H. T. Hewitt, 2013: Identifying uncertainties in Arctic climate change projections. *Climate Dyn.*, **40**, 2849–2865, https://doi.org/10.1007/s00382-012-1512-z.

Hsiang, S., and Coauthors, 2017: Estimating economic damage from climate change in the United States. *Science*, **356**, 1362–1369, https://doi.org/10.1126/science.aal4369.

Iacono, M. J., J. S. Delamere, E. J. Mlawer, M. W. Shephard, S. A. Clough, and W. D. Collins, 2008: Radiative forcing by long-lived greenhouse gases: Calculations with the AER radiative transfer models. *J. Geophys. Res.*, **113**, D13103, https://doi.org/10.1029/2008JD009944.

IPCC, 2014: *Climate Change 2014: Synthesis Report*. R. K. Pachauri and L. A. Meyer, Eds., Cambridge University Press, 151 pp., https://www.ipcc.ch/pdf/assessment-report/ar5/syr/SYR_AR5_FINAL_full.pdf.

Juhola, S., N. Klein, J. Käyhkö, and T. S. Neset, 2017: Climate change transformations in Nordic agriculture? *J. Rural Stud.*, **51**, 28–36, https://doi.org/10.1016/j.jrurstud.2017.01.013.

Krishnan, M., H. T. Nguyen, and J. J. Burke, 1989: Heat shock protein synthesis and thermal tolerance in wheat. *Plant Physiol.*, **90**, 140–145, https://doi.org/10.1104/pp.90.1.140.

Kunreuther, H., and Coauthors, 2014: Integrated risk and uncertainty assessment of climate change response policies. *Climate Change 2014: Mitigation of Climate Change*. O. Edenhofer et al., Eds., Cambridge University Press, 151–205, https://www.ipcc.ch/pdf/assessment-report/ar5/wg3/ipcc_wg3_ar5_chapter2.pdf.

Lader, R., U. S. Bhatt, J. E. Walsh, T. S. Rupp, and P. A. Bieniek, 2016: Two-meter temperature and precipitation from atmospheric reanalysis evaluated for Alaska. *J. Appl. Meteor. Climatol.*, **55**, 901–922, https://doi.org/10.1175/JAMC-D-15-0162.1.

——, J. E. Walsh, U. S. Bhatt, and P. A. Bieniek, 2017: Projections of twenty-first-century climate extremes for Alaska via dynamical downscaling and quantile mapping. *J. Appl. Meteor. Climatol.*, **56**, 2393–2409, https://doi.org/10.1175/JAMC-D-16-0415.1.

Liston, G. E., and C. A. Hiemstra, 2011: The changing cryosphere: Pan-Arctic snow trends (1979–2009). *J. Climate*, **24**, 5691–5712, https://doi.org/10.1175/JCLI-D-11-00081.1.

Unauthenticated | Downloaded 12/28/22 08:07 PM UTC

Matthews, K. B., M. Rivington, K. Buchan, D. Miller, and G. Bellocchi, 2008: Characterising the agro-meteorological implications of climate change scenarios for land management stakeholders. *Climate Res.*, **37**, 59–75, https://doi.org/10.3354/cr00751.

Menne, M. J., I. Durre, R. S. Vose, B. E. Gleason, and T. G. Houston, 2012: An overview of the Global Historical Climatology Network-Daily database. *J. Atmos. Oceanic Technol.*, **29**, 897–910, https://doi.org/10.1175/JTECH-D-11-00103.1.

Miller, P., W. Lanier, and S. Brandt, 2001: Using growing degree days to predict plant stages. Montana State University Publ. MT200103AG, 8 pp., http://msuextension.org/publications/AgandNaturalResources/MT200103AG.pdf.

Monier, E., L. Xu, and R. Snyder, 2016: Uncertainty in future agro-climate projections in the United States and benefits of greenhouse gas mitigation. *Environ. Res. Lett.*, **11**, 055001, https://doi.org/10.1088/1748-9326/11/5/055001.

Morrison, H. C., G. Thompson, and V. Tatarskii, 2009: Impact of cloud microphysics on the development of trailing stratiform precipitation in a simulated squall line: Comparison of one- and two-moment schemes. *Mon. Wea. Rev.*, **137**, 991–1007, https://doi.org/10.1175/2008MWR2556.1.

NOAA/ESRL, 2017: Trends in atmospheric carbon dioxide: Recent monthly average Mauna Loa CO_2. NOAA/ESRL Global Monitoring Division, accessed 15 October 2017, https://www.esrl.noaa.gov/gmd/ccgg/trends/.

NOAA/NWS, 2017: Fairbanks area frost and growing season information. NOAA/NWS Rep., https://www.weather.gov/media/afg/climate/Fairbanks_growing_season.pdf.

Overland, J. E., E. Hanna, I. Hanssen-Bauer, S.-J. Kim, J. E. Walsh, M. Wang, U. S. Bhatt, and R. L. Thoman, 2016: Surface air temperature. NOAA/Arctic Program Rep., https://www.arctic.noaa.gov/Report-Card/Report-Card-2016/ArtMID/5022/ArticleID/271/Surface-Air-Temperature.

Parent, M. B., and D. Verbyla, 2010: The browning of Alaska's boreal forest. *Remote Sens.*, **2**, 2729–2747, https://doi.org/10.3390/rs2122729.

Park, T., and Coauthors, 2016: Changes in growing season duration and productivity of northern vegetation inferred from long-term remote sensing data. *Environ. Res. Lett.*, **11**, 084001, https://doi.org/10.1088/1748-9326/11/8/084001.

Pastick, N. J., M. T. Jorgenson, B. K. Wylie, S. J. Nield, K. D. Johnson, and A. O. Finley, 2015: Distribution of near-surface permafrost in Alaska: Estimates of present and future conditions. *Remote Sens. Environ.*, **168**, 301–315, https://doi.org/10.1016/j.rse.2015.07.019.

Raynolds, M. K., and D. A. Walker, 2016: Increased wetness confounds Landsat-derived NDVI trends in the central Alaska North Slope region, 1985–2011. *Environ. Res. Lett.*, **11**, 085004, https://doi.org/10.1088/1748-9326/11/8/085004.

Riahi, K., and Coauthors, 2011: RCP 8.5—A scenario of comparatively high greenhouse gas emissions. *Climatic Change*, **109**, 33–57, https://doi.org/10.1007/s10584-011-0149-y.

Sánchez, B., A. Rasmussen, and J. Porter, 2014: Temperatures and the growth and development of maize and rice: A review. *Global Change Biol.*, **20**, 408–417, https://doi.org/10.1111/gcb.12389.

Schlenker, W., and M. J. Roberts, 2009: Nonlinear temperature effects indicate severe damages to U.S. crop yields under climate change. *Proc. Natl. Acad. Sci. USA*, **106**, 15 594–15 598, https://doi.org/10.1073/pnas.0906865106.

Skamarock, W. C., and Coauthors, 2008: A description of the Advanced Research WRF version 3. NCAR Tech. Note NCAR/TN-475+STR, 113 pp., https://doi.org/10.5065/D68S4MVH.

Smith, W. N., and Coauthors, 2013: Assessing the effects of climate change on crop production and GHG emissions in Canada. *Agric. Ecosyst. Environ.*, **179**, 139–150, https://doi.org/10.1016/j.agee.2013.08.015.

Soil Survey Staff, 2014: *Keys to Soil Taxonomy.* 12th ed. United States Department of Agriculture/Natural Resources Conservation Service, 372 pp.

——, 2017: Web Soil Survey. United States Department of Agriculture/Natural Resources Conservation Service, accessed 13 October 2017, http://websoilsurvey.nrcs.usda.gov/.

Unauthenticated | Downloaded 12/28/22 08:07 PM UTC

Taylor, K. E., R. J. Stouffer, and G. A. Meehl, 2012: An overview of CMIP5 and the experiment design. *Bull. Amer. Meteor. Soc.*, **93**, 485–498, https://doi.org/10.1175/BAMS-D-11-00094.1.

Thoman, R., and T. Fathauer, 1998: An investigation into estimating greenup dates around Fairbanks Alaska using thermal indices. *Proc. 49th Arctic Science Conf.*, Fairbanks, AK, University of Alaska Fairbanks, 14 pp.

Tripathi, A., D. K. Tripathi, D. K. Chauhan, N. Kumar, and G. S. Singh, 2016: Paradigms of climate change impacts on some major food sources of the world: A review of current knowledge and future prospects. *Agric. Ecosyst. Environ.*, **216**, 356–373, https://doi.org/10.1016/j.agee.2015.09.034.

USDA/NASS, 2014a: 2012 Census of Agriculture: Alaska state and area data. United States Department of Agriculture/National Agricultural Statistics Service, accessed 14 June 2017, https://www.agcensus.usda.gov/Publications/2012/Full_Report/Volume_1,_Chapter_1_State_Level/Alaska/akv1.txt.

——, 2014b: 2012 Census of Agriculture: Alaska county-level boundaries. United States Department of Agriculture/National Agricultural Statistics Service, accessed 14 June 2017, http://www.agcensus.usda.gov/Publications/2012/Online_Resources/Ag_Atlas_Maps/mapfiles/CoGenAll_GCS12.zip.

Van Veldhuizen, R. M., and C. W. Knight, 2004: Performance of agronomic crop varieties in Alaska 1978–2002. *AFES* Bulletin, Vol. 111, 136 pp., https://scholarworks.alaska.edu/bitstream/handle/11122/1310/Bulletin111.pdf?sequence=1.

Wahid, A., S. Gelani, M. Ashraf, and M. R. Foolad, 2007: Heat tolerance in plants: An overview. *Environ. Exp. Bot.*, **61**, 199–223, https://doi.org/10.1016/j.envexpbot.2007.05.011.

Wendler, G., and M. Shulski, 2009: A century of climate change for Fairbanks, Alaska. *Arctic*, **62**, 295–300, https://doi.org/10.14430/arctic149.

Yu, Q., Y. Zhang, Y. Liu, and P. Shi, 2004: Simulation of the stomatal conductance of winter wheat in response to light, temperature and CO_2 changes. *Ann. Bot.*, **93**, 435–441, https://doi.org/10.1093/aob/mch023.

Zhang, X., and J. Zhang, 2001: Heat and freshwater budgets and pathways in the Arctic Mediterranean in a coupled ocean/sea-ice model. *J. Oceanogr.*, **57**, 207–234, https://doi.org/10.1023/A:1011147309004.

Earth Interactions is published jointly by the American Meteorological Society, the American Geophysical Union, and the Association of American Geographers. For information regarding reuse of this content and general copyright information, consult the AMS Copyright Policy (www.ametsoc.org/PUBSReuseLicenses).

Unauthenticated | Downloaded 12/28/22 08:07 PM UTC